

Comparison of the osteoblastic activity of low elastic modulus Ti-24Nb-4Zr-8Sn alloy and pure titanium modified by physical and chemical methods

Xinxin Zhan^{a,f}, Shujun Li^b, Yuntao Cui^c, Anqi Tao^a, Chengcheng Wang^a, Huazhi Li^a,
Linlin Zhang^d, Hanrong Yu^d, Jiuhui Jiang^{a,*}, Cuiying Li^{e,*}

^a Department of Orthodontics, Peking University School and Hospital of Stomatology, #22 Zhongguancun South Avenue, Haidian District, Beijing 100081, China

^b Titanium Alloy Laboratory, Institute of Metal Research, Chinese Academy of Sciences, #72 Wenhua Road, Shenyang 110016, China

^c CAS Key Laboratory of Cryogenics and Beijing Key Laboratory of Cryo-Biomedical Engineering, Technical Institute of Physics and Chemistry, Chinese Academy of Sciences, Beijing 100190, China

^d Department of Dental Implants, Affiliated Stomatological Hospital of Jiamusi University, Jiamusi, China

^e Central Laboratory, Peking University School and Hospital of Stomatology, #22 Zhongguancun South Avenue, Haidian District, Beijing 100081, China

^f National Engineering Laboratory for Digital and Material Technology of Stomatology, Beijing, China

ARTICLE INFO

Keywords:

Low elastic modulus Ti-24Nb-4Zr-8Sn alloy
Bioactivity of bone marrow mesenchymal stem cells
Sandblasted, large-grit, acid-etched
Micro-arc oxidation
Anodic oxidation

ABSTRACT

Ti-24Nb-4Zr-8Sn (Ti2448) alloy is a novel low elastic modulus β -titanium alloy without toxic elements. It also has the advantage of high strength, so it has potential application prospects for implantation. To develop its osteogenic effects, it can be modified by electrochemical, and physical processes. The main research aim of this study was to explore the bioactivity of Ti2448 alloy modified by sandblasted, large-grit, acid-etched (SLA), micro-arc oxidation (MAO) and anodic oxidation (AO), and to determine which of the three surface modifications is the best way for developing the osteogenesis of bone marrow mesenchymal stem cells (BMMSCs). In vitro studies, the cytoskeleton, focal adhesion and proliferation of BMMSCs showed that both pure titanium and Ti2448 alloy have good biocompatibility. The osteogenic differentiation of BMMSCs with the Ti2448 alloy were examined by detecting alkaline phosphatase (ALP), mineralization nodules and osteogenic proteins and were better than that with pure titanium. These results showed that the Ti2448 alloy treated by SLA has a better effect on osteogenesis than pure titanium, and AO is the best way of three surface treatments to improve osteogenesis in this study.

1. Introduction

Implant restoration provides hope for patients with edentulous, greatly improves the masticatory efficiency and quality of life of these patients after restoration. However, there are still some problems, such as partial bone resorption, poor stress effect after implantation, etc. [1]. The causes of these problems are related to the patient's own physical condition, living habits such as smoking, surgical methods and implant material [2,3]. Among them, implant prostheses have high requirements for implant material [4]. On the one hand, the material needs good biocompatibility, such as no cytotoxicity, no release of toxic elements into the body, and no serious immuno-inflammatory responses. On the other hand, it is expected that implant material should closely combine with bone tissue, rather than wrap by fibrous tissue [5]. The stress shielding effect should not be neglected after an implant is loaded [6–8]. In response to the above requirements, pure titanium, titanium

alloys and the other metal materials have been widely used as implant material because of their good mechanical properties [9]. However, due to the stable physical and chemical properties of titanium alloys in an air environment, it is not easy to guide bone tissue to grow on their surfaces [10,11]. Therefore, surface modifications of metal materials, such as mechanical sandblasting, mechanical cutting; physical and chemical methods, such as micro-arc oxidation and alkali heatment; and biological methods, such as surface adsorption of proteins, enzymes molecules, etc. [12–14], have been used to solve this problem. Furthermore, the improved electrochemical processes, such as plasma electrolytic oxidation (PEO) and magnetoelectropolishing (MEP), which were researched by Krzysztof Rokosz et al. [15–17], Ryszard Rokicki et al. [18–21], and Tadeusz Hryniewicz et al. [18–20], have also been identified to promote cell adhesion and proliferation [21]. Electrochemical methods could improve the surface bioactivity of metal materials. After surface modification, the surface biological activity of

* Corresponding authors.

E-mail addresses: drjiangw@163.com (J. Jiang), Licuiying_67@163.com (C. Li).

<https://doi.org/10.1016/j.msec.2020.111018>

Received 26 September 2019; Received in revised form 13 April 2020; Accepted 24 April 2020

Available online 25 April 2020

0928-4931/ © 2020 Elsevier B.V. All rights reserved.

pure titanium and titanium alloys has been improved [22].

The elastic modulus of pure titanium is proximately 107 GPa, and that of titanium alloys such as Ti-6Al-4V is about 117 GPa, while the elastic modulus of bone cortex is proximately 20 GPa [23]. Because the elastic modulus of these implant materials and bone tissue does not match, a stress shielding effect will occur, which will lead to adverse effects such as bone resorption [24]. The elastic modulus of Ti-24Nb-4Zr-8Sn alloy with ultimate tensile strength (~950 MPa) is proximately 49 GPa, which is lower than the elastic modulus of the implant metal materials currently used and closer to that of bone tissue [25–29]. The matching between the elastic modulus of implant material and the surrounding bone tissue is an important factor for successful implant implantation [30–33]. The elastic modulus of the implant materials used at present is higher than that of bone tissue, which is prone to stress shielding effects and increases the risk of bone resorption. Ti2448 alloy has a high strength and lower elastic modulus than pure titanium [25,34]. Because of these mechanical properties, it has the potential to be used in clinical practice, and probably better than pure titanium [35–37]. Current research showed that the main elements of Ti2448 alloy are Ti, Nb, Zr and Sn; elemental toxicity of elements is in the order $Ag^+ > Au^{3+} > Cu^{2+} > Co^{2+} > Pd^{2+} > Cr^{3+} > In^{3+} > Sn^{2+}$ [38]. The elements in Ti2448 alloy will not have great toxicity in the body, nor will the alloy produce an immune reaction or allergy. K.C. Nune et al. performed experiments in vitro that showed that Ti2448 alloy has good biological activity and osteoblast activity, and has potential application in implants [39]. To improve the biological response of Ti2448 alloy to bone tissue, surface modification was carried out, for example, changing the surface structure to a mesh structure [40] and modifying the structure by micro-arc oxidation and anodic oxidation under different conditions [41–48]. The osteoblast activity was promoted by changing the surface morphology and chemical composition.

It has been shown that the activity of osteoblasts was improved after surface modification, but few surface modification methods have been used on Ti2448 alloy, and it cannot be determined that which method of Ti2448 alloy surface modifications is the best. To compare the surface physical and chemical properties of Ti2448 alloy with those of pure titanium under different treatment conditions, both substrates were treated by sandblasted, large-grit, acid-etched (SLA), micro-arc oxidation (MAO) and anodic oxidation (AO). Then, we discussed the factors affecting the cell biological activity and cell differentiation, observed the bioactivity effect of Ti2448 alloy and explored which method is best for osteogenesis.

2. Materials and methods

2.1. Preparation and surface modification of pure titanium and Ti2448 alloy

Samples with diameters of 10 mm or 25 mm and thicknesses of 1.5 mm were prepared and modified by SLA, MAO and AO. The substrates of commercial grade 4 pure titanium (TA4) (provided by Jiangsu Trausim Medical Instrument Company, China) and Ti2448 alloy (provided by Institute of Metal Research, Chinese Academy of Sciences, China) were cut into pieces with dimensions of 10 mm and 25 mm, and a thickness of 1.5 mm (WEDM, DK7732, Yinuo Machine Tool Manufacturing Co., Ltd., Guangdong, China). Then, the surface was polished to a metallic luster (Polishing machine, PG40, Wuxi Taiyuan Machine Manufacturing Co., Ltd., China) and dried (Electric constant temperature blast drying oven, 101-A, Huyueming Scientific Instrument Co., Ltd., Shanghai, China) after ultrasonic cleaning (XR-1015-25A, Xinren ultrasonic equipment Co., Ltd., Jiangsu, China). After the pure titanium and Ti2448 alloy samples were cut, polished, cleaned and dried according to the operation method of the machining group, the first group of samples was sandblasted (Automatic Sandblasting Machine, 9060B, Jianhui mechanical equipment Co., Ltd., Jiangsu, China) with white corundum (Al_2O_3), particles size of 60 mesh as the

sandblasting medium, 3–4 bar sandblasting pressure and about 10 s sandblasting time. Then, these samples were placed in a mixture of 9.4 mol/L sulfuric acid and 0.5 mol/L hydrochloric acid solution for 30 min at 40 °C, followed by ultrasonic cleaning and drying. Micro-arc oxidation was carried out (WHD20, micro-arc oxidation equipment, Harbin University of technology Sino Russian science and Technology Research Cooperation Co., Ltd., China) at 250 V for 10 min with immersing in alkaline calcium phosphate solution, and ultrasonic cleaning was performed again before drying. Anodic oxidation is an electrochemistry process in which the voltage is 30 V and the substrates were placed in a 1 mol/L NH_4SO_4 and 0.15 mol/L NH_4F solution for 2 h. Before cell seeding on the samples, all samples were ultrasonically cleaned in the acetone, isopropanol, ethanol and deionized water for 10 min successively and autoclaved. The specimens were steam sterilized at 121 °C for 20 min and dried at 70 °C for 15 min.

2.2. Material characterizations

A scanning electron microscope (JSM-IT300, JEOL, Japan) was used to explore the morphological characteristics of all material surfaces to identify their differences. The X-ray photoelectron spectrometer (AXIS Supra, Kratos Analytical Ltd., England) was used to analyze the chemical elements on the surfaces of modified pure titanium and Ti2448 alloy. The roughness of the materials was evaluated in terms of Ra by three-dimensional morphometry laser microscopy (VK-X200, Keyence, Japan) according to the DIN EN ISO 4287 standard. The hydrophilicity of the modified material surfaces was analyzed by the contact angle measurement with a drop shape analyzer (Kruss DSA100, Germany). The characteristics of the modified pure titanium and Ti2448 alloy were compared to explore their differences. The coatings on the sides of pure titanium and Ti2448 alloy samples modified by micro-arc oxidation and anodic oxidation were removed with conductive adhesive, and the cross sections of the coatings were exposed. Field emission scanning electron microscopy (Hitachi SU8010, Japan) was used to observe the thickness of the MAO and AO coatings.

2.3. Cell culture

Human bone marrow mesenchymal stem cells (HBMSCs, Science Cell Research Laboratories, California, USA) were cultured at 5% CO_2 and 100% humidity in alpha-modified minimum essential medium (α -MEM, Gibco, USA) containing 10% fetal bovine serum (FBS, Gibco, Australia). The fourth to sixth generation cells were chosen to mix into cell suspensions and then seeded on Ti2448 alloys and pure titanium at a density of 1×10^4 cells/mL. According to the research designs, the cells were cultured for different incubation periods, and then the specific experimental schemes were carried out.

2.4. Cell proliferation

The activity of osteoblasts cultured on the surfaces of the materials was evaluated, and cell proliferation was detected using CCK-8 kits (Dojindo Molecular Technologies, Japan). BMSCs were seeded onto the samples, and cell proliferation was detected at set time. Then, the sheets were washed and transferred to a new 48-well plate at the selected incubation periods. The culture medium was mixed with cck-8 reagent at a ratio of 10:1. Then, 500 μ L CCK-8 detection solution was put into each well. After 2 h of incubation in a 5% CO_2 incubator at 37 °C, the solution in each well was transferred to a 96-well plate, 100 μ L per well. The optical density (OD) value was measured using an ELISA reader (Biotek, ELX808, USA) at 450 nm.

2.5. Immunofluorescence of cytoskeletal actin and vinculin

The intracellular proteins vinculin and actin were observed by immunofluorescence microscopy to study cells morphology and motility.

After 24 h of incubation, the cells on the surface of the materials were fixed with 4% paraformaldehyde at 4 °C for 15 min. The sheets were washed with PBS after each subsequent step at room temperature. The cells were blocked with 1% bovine serum albumin in PBS after permeation with 0.1% Triton X-100 in PBS. Cells were incubated overnight with diluted primary antibody (anti-vinculin) (1:200), subsequently labeling them with diluted secondary antibody (1:100) (goat-anti-mouse FITC conjugate) (ASGB-BIO, China) for 30 min, and then incubating them with diluted phalloidin FITC solution (1:400) (Sigma-Aldrich, USA) for 40 min. Finally, nuclei were labeled with DAPI (ASGB-BIO, China). After immunostaining, the cells were examined by laser scanning confocal microscopy (Carl Zeiss, Germany).

2.6. Differentiation and mineralization assay

Quantitative analysis of alkaline phosphatase (ALP) was used to detect early osteogenic differentiation of BMSCs cultured on the surfaces of the samples for 7 days using an ALP assay kit (Njcbio, China). The absorbance at 520 nm was measured via spectrophotometry with a multimode plate reader (PerkinElmer, Singapore). To study the effect of ECM mineralization on bone formation, qualitatively and quantitative alizarin red analysis of calcium mineralization in the matrix were carried out. After cells were cultured for 21 days, the samples were fixed with 4% paraformaldehyde for 15 min. After washing with deionized water, the samples were stained with alizarin red (Sigma, USA) (1% w/v) solution in deionized water. The specimens were scanned by a scanner (HP Scanjet, G4050, USA). To detect the degree of mineralization quantitatively, 10% cetyl-pyridinium chloride (CPC) was added to dissolve the red matrix sediment. The absorbance of the solution was measured at 490 nm OD with a multimode plate reader (PerkinElmer, Singapore).

2.7. Osteogenic protein factors expression

After incubation for 21 days, the cells on the samples were collected to extract the total protein. Then, bone morphogenetic protein (BMP-2), runt-related transcription factor 2 (Runx2), and osteocalcin (OCN) were inspected using a human BMP-2 ELISA kit (Raybiotech, USA), a human runt-related transcription factor 2 ELISA Kit (Abbkine, USA) and a human osteocalcin quantitative ELISA kit (R&D Systems, USA), respectively. The absorbance of the solution was measured with an ELISA reader (Biotek, ELX808, USA) according to specifications.

2.8. Statistical analysis of data

A one-way analysis of variance (ANOVA) was used to analyze the data. A p value < 0.05 was considered significant. Statistical analysis was performed using GraphPad Prism software (San Diego, CA, USA).

3. Results

3.1. The surface characterizations of modified pure titanium and Ti2448 alloy

The surface topographies of pure titanium and Ti2448 alloy modified by SLA, MAO and AO were characterized by SEM, as shown in Fig. 1. The surfaces of both machined pure titanium and Ti2448 alloy (a, e) showed regular stripes. After treatment by SLA, the surface of the Ti2448 alloy (f) contained pits, while that of pure titanium (b) contained peaks and valleys. The surfaces of both substrates modified by micro-arc oxidation were pore shaped, but the diameters of the pores were different, approximately 1 μm on pure titanium (c) and approximately 3 μm on Ti2448 alloy (g). The area occupied by pores for Ti-MAO was 0.14%, for Ti2448-MAO was 8.78% according to the corresponding image J's images of Ti-MAO and Ti2448-MAO. It was also found that the larger the number of pores, the smaller the pores area

[49]. Nanotube structures formed distinctly on the surface of Ti2448 alloy treated by AO (h), the diameter of the nanotube is approximately 100 nm, and surface uneven, part of the nanotubes raised, part of the nanotubes sunk. However, nonregular nanopores formed on the surface of pure titanium at 30 V (d). According to previous research [43], when the anodic oxidation voltage is 30 V, cells can better adhere to the surface of materials, which increases the differentiation potential of cells. Therefore, a 30 V constant voltage direct current was selected.

As shown on the surface altitude chart and by the Ra values (Fig. 2), the surface roughnesses of pure titanium and Ti2448 alloy were all increased after surface modification. In addition, the anodized surface roughness of Ti2448 alloy was the highest. The Ra values of both machined surfaces were < 0.5 μm, the Ra values of Ti-SLA, Ti-MAO and Ti2448-SLA were 1 μm–2 μm, and Ra values of the rest surfaces were > 2 μm.

The contact angles were detected by a contact goniometer. The surface of the nanostructures with good hydrophilicity is conducive to the biological reaction of osteoblasts [50]. As shown in the Fig. 3, the pure Ti and Ti2448 alloy modified by AO have higher hydrophilicity. The surface contact angles of pure Ti and Ti2448 alloy decreased after treated by SLA, and that of pure Ti increased after modified by MAO. The contact angle is closely related to the surface topography.

XPS spectra (Fig. 4) showed that there were oxides on the surfaces of pure titanium and Ti2448 alloy modified by SLA, MAO and AO. Through the analysis of elemental oxides, the surface oxide of Ti-M and Ti-SLA is TiO₂, and that of Ti2448-M and Ti2448-SLA are TiO₂, ZrO₂, SnO and Nb₂O₅. After the micro-arc oxidation treatment, CaO and Ca₃(PO₄)₂ can be observed on the surface of Ti-MAO, and Ca₃(PO₄)₂ on the surface of Ti2448-MAO.

Among all surface treatment methods, the material surfaces after micro-arc oxidation and anodic oxidation treatment formed coatings, and the layer thickness is shown in Fig. 5. Measured by ImageJ, the thicknesses of Ti-MAO, Ti-AO, Ti2448-MAO and Ti2448-AO were approximately 11 μm, 6 μm, 18 μm and 8 μm respectively. The results showed that the MAO coatings are thicker than the AO coatings. The thickness of the coating may be also related to the substrate material. The thickness of the surface coating of Ti2448 alloy was higher than that of pure Ti. In addition, as shown in Fig. 5, the boundary between the micro-arc oxidation coating and the substrate material is fuzzy, while the boundary between the anodic oxidation coating and the substrate material is clear, or even separated, so the bonding strength between the micro-arc oxidation coating and the substrate may be stronger.

3.2. Cell proliferation and bioactivity test

The cell proliferation on the Ti-M, Ti-SLA, Ti-MAO, Ti-AO, Ti2448-M, Ti2448-SLA, Ti2448-MAO and Ti2448-AO samples was measured by CCK-8 assay, and results showed that the cells continued to proliferate on all surfaces from first day to 8th day (Fig. 6). In this study, the cell proliferation of the MAO group was higher than that of the other groups. Between pure titanium and Ti2448 alloy, the cell proliferation on the surfaces of Ti2448 alloy was higher. Roughness increased, the proliferation of osteoblasts decreased [51], but that of osteoblasts on the MAO surface increased.

After incubated for 1 day, the cytoskeleton, vinculin and nuclei of BMSCs grown on the Ti2448 alloys and pure titanium modified by different methods were observed by laser scanning confocal microscopy. The cytoskeleton morphologies on titanium samples with different microstructures shown in Fig. 7 are different. The BMSCs on the machined Ti and Ti2448 alloy were flattened regularly and grew along the stripes of the machined surfaces, whereas the morphologies of BMSCs on the SLA, MAO and AO surfaces were more spread out, and the cells grew irregularly. Compared to the cells on the AO and SLA sample surfaces, BMSCs on the MAO sample surface seemed to show more F-actin filament aggregation sites. Comparing the cells on the

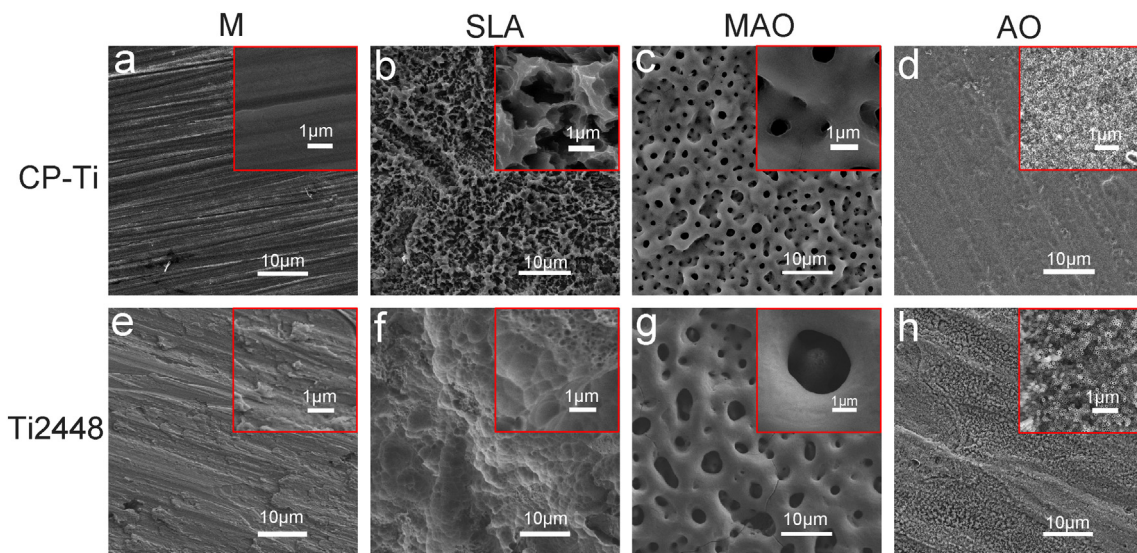


Fig. 1. Surface morphology of treated pure titanium and Ti2448 alloy. The microstructure of surface morphology were observed on CP-Ti (a–d) and Ti2448 alloy (e–h) using SEM.

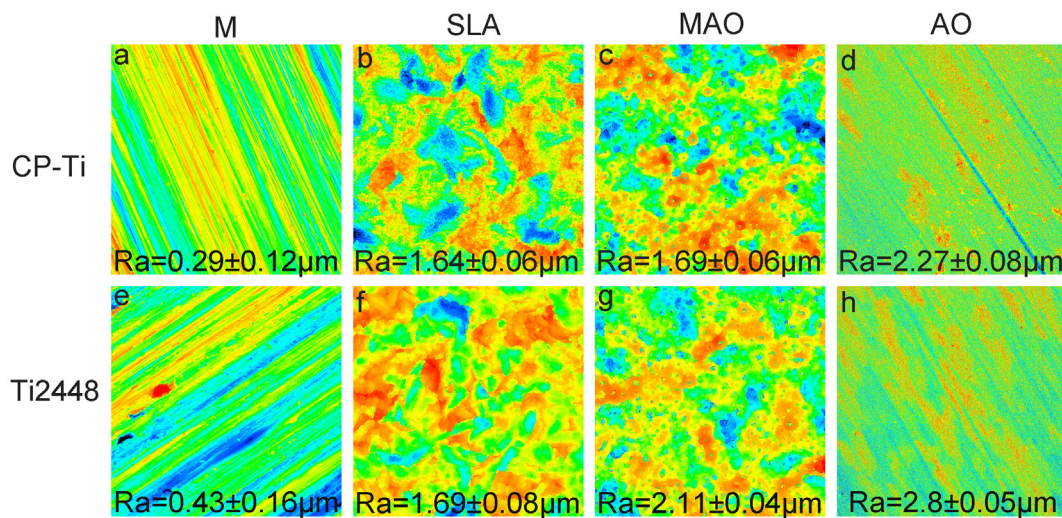


Fig. 2. Surface roughness of pure Ti and Ti2448 alloy. Surface roughness of the Ti samples: (a) Ti-M, (b) Ti-SLA, (c) Ti-MAO, (d) Ti-AO and Ti2448 alloy; (e) Ti2448-M, (f) Ti2448-SLA, (g) Ti2448-MAO and (h) Ti2448-AO were determined by three-dimensional morphometry laser microscopy.

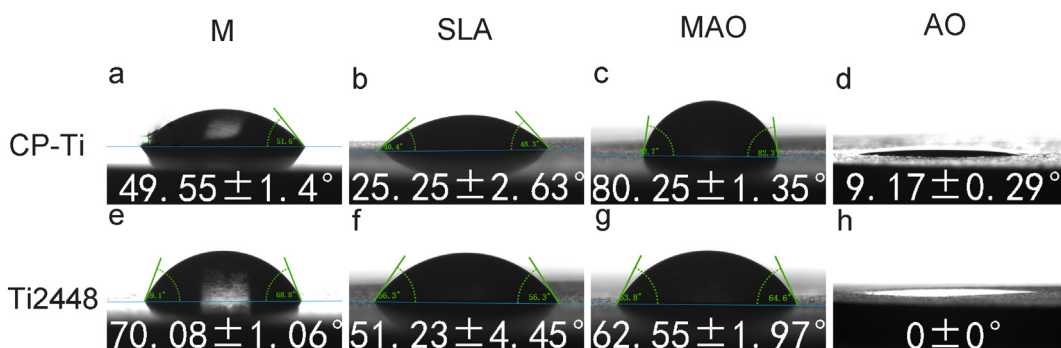


Fig. 3. The hydrophilicity of machined and SLA-, MAO-, AO-treated Ti and Ti2448 alloy. Contact angles of the anodized samples (d, h) are significantly less than those of the other samples.

surfaces of Ti-AO and Ti2448-AO, the cytoskeleton of BMMSCs on the Ti2448-AO sample was more clearly visible.

3.3. The differentiation of BMMSCs and extracellular matrix mineralization

To verify the difference between the differentiation and

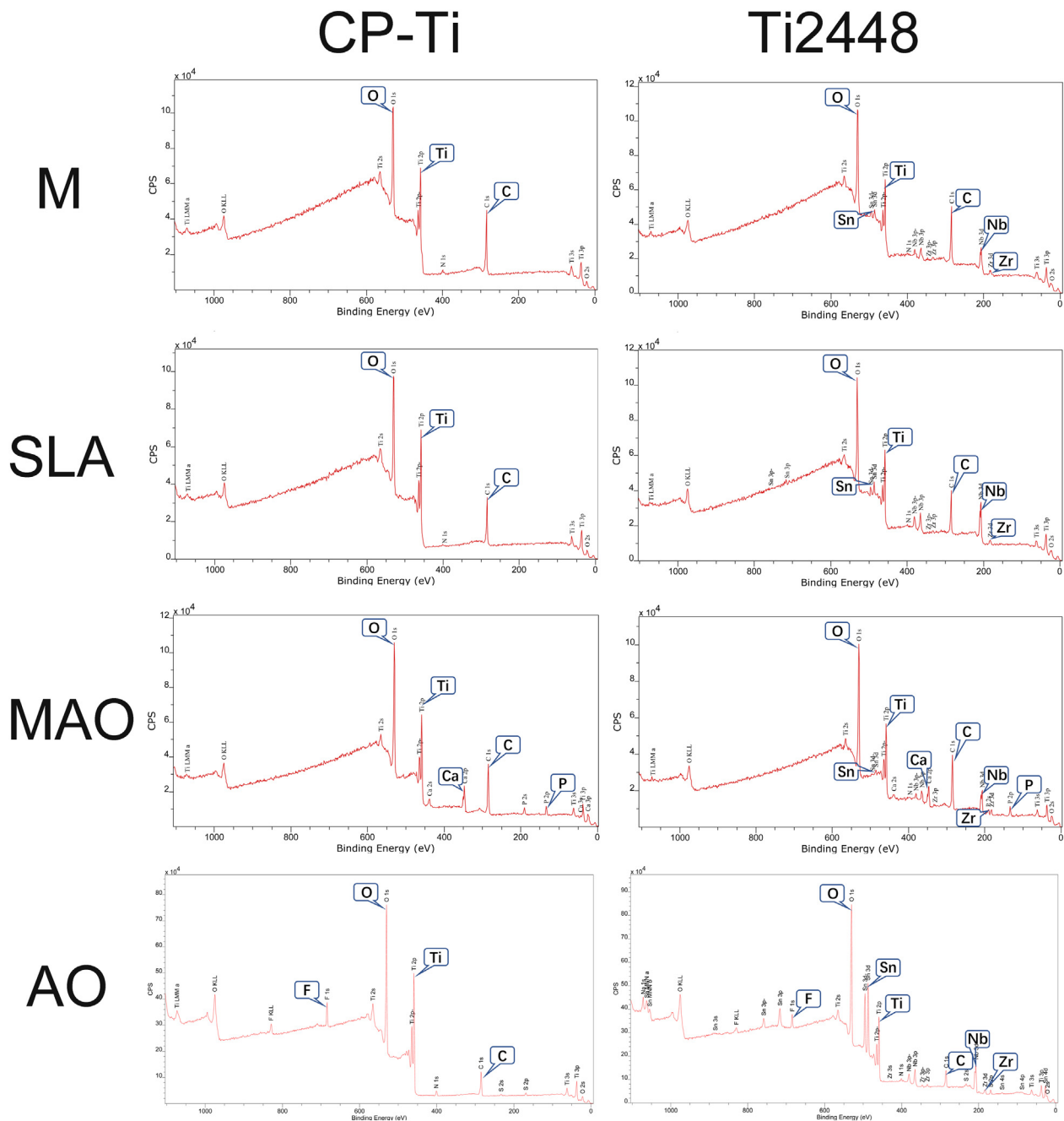


Fig. 4. XPS spectra of pure titanium and Ti2448 alloy modified by SLA, MAO and AO. The element composition on the different surfaces of pure titanium and Ti2448 alloy.

mineralization of osteoblasts on surface-treated Ti2448 alloy and pure titanium, alkaline phosphatase (ALP) was used to detect the early osteogenic effect [52]. Alizarin red staining was analyzed qualitatively and quantitatively to observe the late osteogenic effect.

After osteoinduction for 7 days, ALP activity was detected using an AKP kit. As shown in Fig. 8, the ALP activities of both substrates modified by MAO and AO were better than that of the machined and SLA groups, and that of BMMSCs on the Ti2448-AO sample was best. The effect of matrix mineralization of the BMMSCs cultured on the eight samples is shown in Fig. 9(A, B). After osteoinduced for 21 days, the mineralized nodules formed on the AO surfaces of both materials obviously increased. In addition, matrix mineralization of osteoblasts on the modified Ti2448 alloy was relatively higher than that on modified pure titanium.

3.4. Osteogenic proteins expression of osteoblasts

BMP-2, OCN and Runx2 proteins were detected to illustrate the influence of cell osteogenic differentiation [53]. As shown in Fig. 10(A) histogram, after osteogenesis induction for 21 days, the expression of OCN on the surface of the two substrates after anodic oxidation was highest in all groups. The expression of OCN on Ti2448-SLA surface was higher than that on pure titanium treated by SLA. There was no significant difference in the expression of OCN between the other groups, which was basically consistent with the alizarin red staining results. The protein expression of BMP-2 and Runx2 were shown in the B and C histograms, respectively. The results showed that the expression of BMP-2 and Runx2 in the anodic oxidation group was lower than that in other groups, but these two proteins expression on the Ti2448-SLA alloy surface was higher than that on the pure Ti-SLA surface.

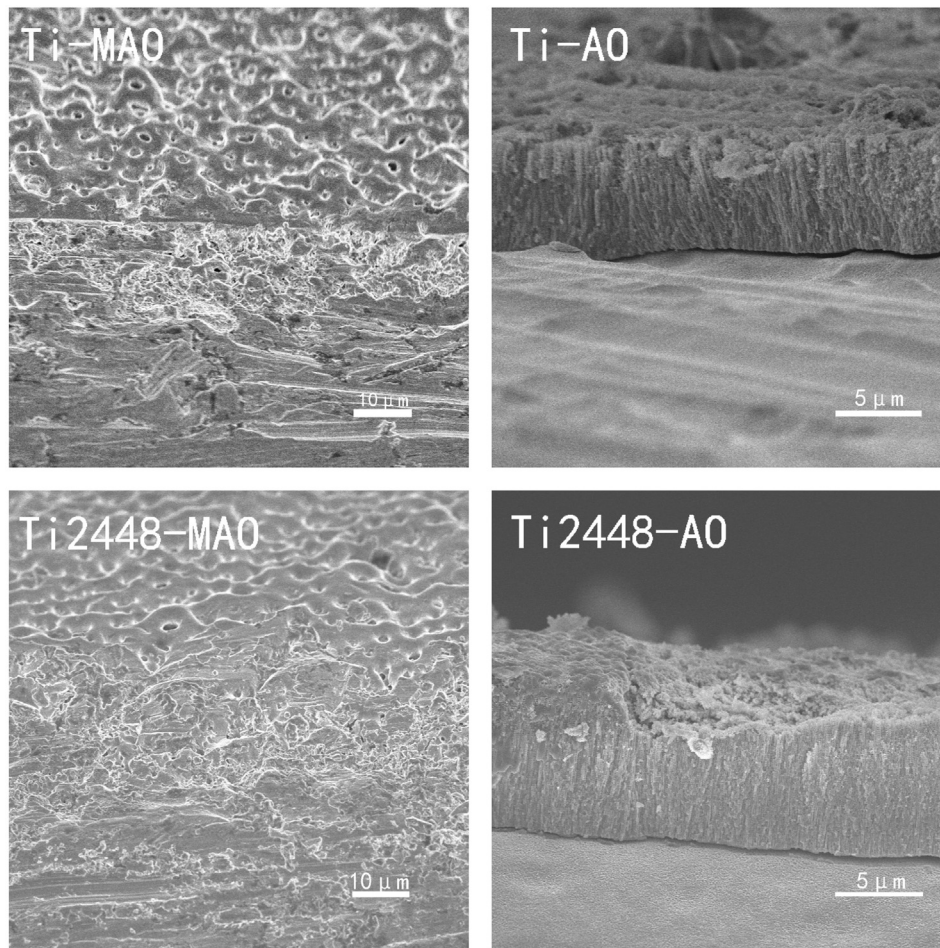


Fig. 5. The thickness of MAO and AO coatings by Field Emission Scanning Electron Microscopy. Ti-MAO and Ti2448-MAO were observed at 1000 \times , and AO coating was observed at 3000 \times .

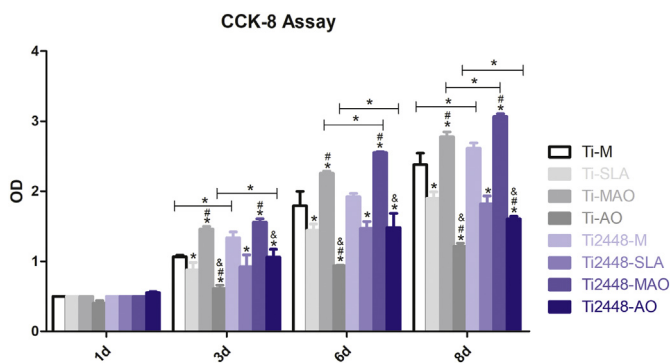


Fig. 6. The proliferation of BMMSCs on the surface of eight group samples. Values are presented as mean \pm SD for different cultures. * $p < 0.05$ versus Ti-M and Ti2448-M; # $p < 0.05$ versus Ti-SLA and Ti2448-SLA; & $p < 0.05$ versus Ti-MAO and Ti2448-MAO.

4. Discussion

The successful implant is based on the formation of osseointegration. The premise of osseointegration is that the surface of the implant material has good biological activity, which is conducive to the formation of bone. Bone formation is related to implant materials, structural design and surface characteristics [54]. To further promote the effect of bone formation, surface modification was carried out on the implant materials [12–14]. And the surface characteristics of the implant materials, such as surface morphology, wettability, and

roughness, changed. The surface morphology affected the hydrophilicity and roughness of the material surface. Researches showed that the better hydrophilicity is conducive to cell adhesion, and the effect of nano or micro surface on cell response is different [55]. The surface oxides and surface topography of materials can affect cell signal transduction, which changes the mode of cell adhesion and spread [56,57]. After modification by physical and chemical methods, some oxides were observed on the surfaces of pure titanium and Ti2448 alloy, the surface activities of metal materials could be increased, and the hydrophilicity of metal material surface could be improved. Then, the adhesion and growth of cells on the material surface can be developed, and cell differentiation can be advanced, which is more conducive to the bonding of bone tissue to a material surface [58–60].

In our study, scanning electron microscopy (SEM) images showed that nanotube structures were formed on the anodized surface, and hydrophilicity detected by drop shape analyzer was the best. The SEM results also showed that a microscale structure formed on the surface of the sandblasted and micro-arc oxidation samples. In some studies [42,51,61,62], Ra value was used as the measurement parameter of surface roughness, and Manuela Galati et al. [63] also said that the arithmetic average value (Ra) could be used as descriptor for surface roughness, so Ra value was applied to compare surface roughness in our study. In the [61] research, the Ra value of the optimal surface roughness is about 2.1–3.1 μm , and Andreas Schedle etc. elucidated that surface with Ra roughness values of 1–2 μm may be optimal for osteoblast differentiation. Obviously, the Ra roughness values in all samples of our research are lower than 3 μm . Some studies [64,65] also concluded that less average peri-implant bone loss around the less

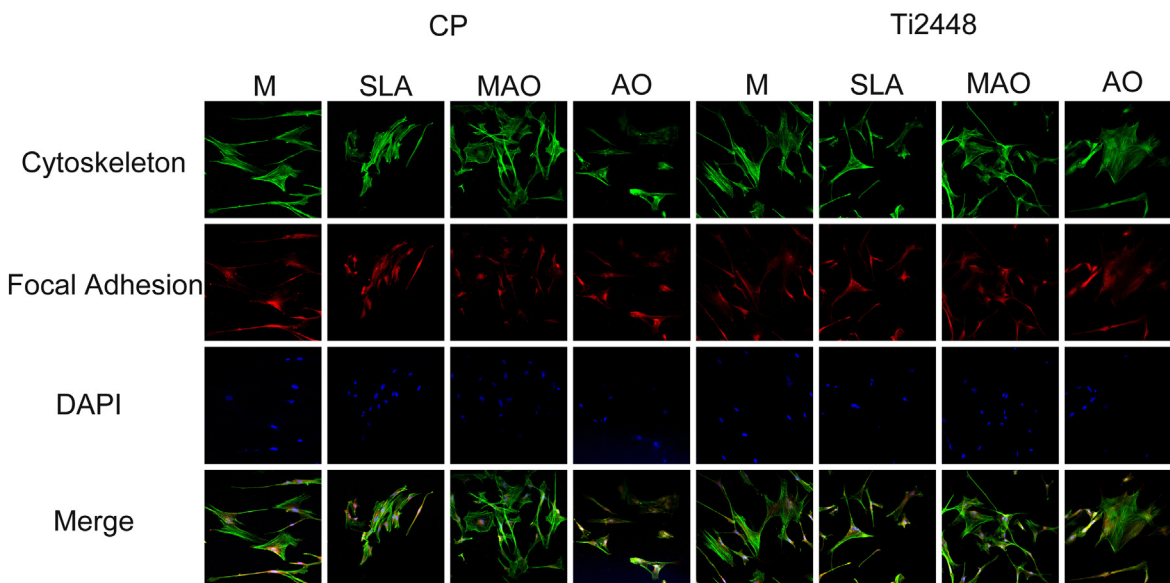


Fig. 7. The morphologies of BMSCs attached to samples observed by laser confocal microscopy. The cytoskeleton is stained green by FITC-Phalloidin, the vinculin is stained red by vinculin antibody, and the nuclei are stained blue by DAPI. (For interpretation of the references to colour in this figure legend, the reader is referred to the web version of this article.)

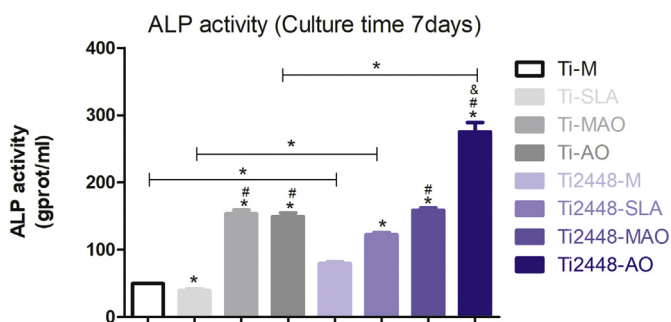


Fig. 8. In vitro ALP activity of BMSCs on samples in the eight groups. Values are presented as mean \pm SD for eight independent cultures. * $p < 0.05$ versus Ti-M and Ti2448-M; # $p < 0.05$ versus Ti-SLA and Ti2448-SLA; & $p < 0.05$ versus Ti-MAO and Ti2448-MAO.

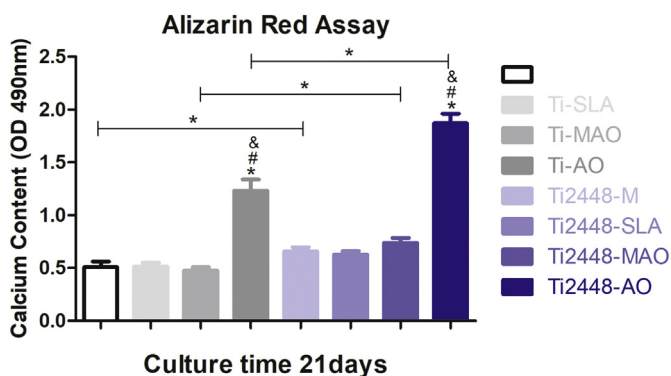


Fig. 9. Qualitative (A) and quantitative (B) analysis of cell mineralization on samples in eight groups. Values are presented as mean \pm SD for eight independent cultures. * $p < 0.05$ versus Ti-M and Ti2448-M; # $p < 0.05$ versus Ti-SLA and Ti2448-SLA; & $p < 0.05$ versus Ti-MAO and Ti2448-MAO.

rough surfaces. But in the review of Tomas Albrektsson [66], bone attraction surface modification is more important for bone formation, and considered to be the only way to improve the clinical success rate.

Following our research, after the biocompatibility test, the results of Figs. 6 and 7 showed that increased roughness is detrimental to the

proliferation of cells [67], but the cell proliferation and cytoskeleton on the surface of pure Ti-MAO and Ti2448-MAO with different Ra values were good, this may be influenced by the surface morphology. These results indicated that the surface of micro-arc oxidation is beneficial to cell growth and adhesion. An irregular surface morphology can be produced after sandblasting and acid etching, enlarging the contact area between the cells and the material surface and increasing the surface roughness, which is beneficial to the differentiation of BMSCs [68]. Early bone formation results showed that the ALP activity of both materials surface increased with the increase of roughness. The results of late cell mineralization showed that the mineralization nodules on anodized surface were especially obvious. The expression of osteogenic protein factors was also consistent with the mineralized nodules. The results showed that the increase of roughness was beneficial to the early osteogenic differentiation of BMSCs, and the nanostructured surface may be most beneficial to the amount of final bone formation. Compared with the bioactivity of the two materials, Ti448 alloy, such as Ti2448-SLA and Ti2448-AO, showed some advantages in various aspects.

In addition to the effect of the surface morphology on cell viability, the oxides of the surface of a material may also be an important factor in promoting cell osteogenic activity. Compared with Ti-M surface, the physical and chemical properties of Ti2448-M surface showed that the surface morphology is similar, the surface roughness is higher, but the hydrophilicity is worse. XPS results showed that the oxides on the surface of Ti2448-M are TiO₂, ZrO₂, SnO and Nb₂O₅, while the main oxide of Ti-M is TiO₂. Previous studies indicated that Nb-based films may have a good effect on promoting bone formation [64]. Some studies also noted that the addition of SnO₂ could effectively promote osteogenic effects [65]. In our research, the cell proliferation and adhesion of Ti2448-M surface were slightly better than that of Ti-M, the difference was not statistically significant, indicating that the biocompatibility of pure titanium and Ti2448 alloy was similar. The results of cell differentiation showed that Ti2448-M surface was more favorable for cell differentiation.

In vitro, surface treatments with micro-arc oxidation and anodization can promote bone formation better than sandblasting and etching, or the surfaces of MAO and AO can be called as bone attraction surface [58]. This may be related to the oxides on the surface of pure titanium and Ti2448 alloy modified by MAO and AO. However, the formation of

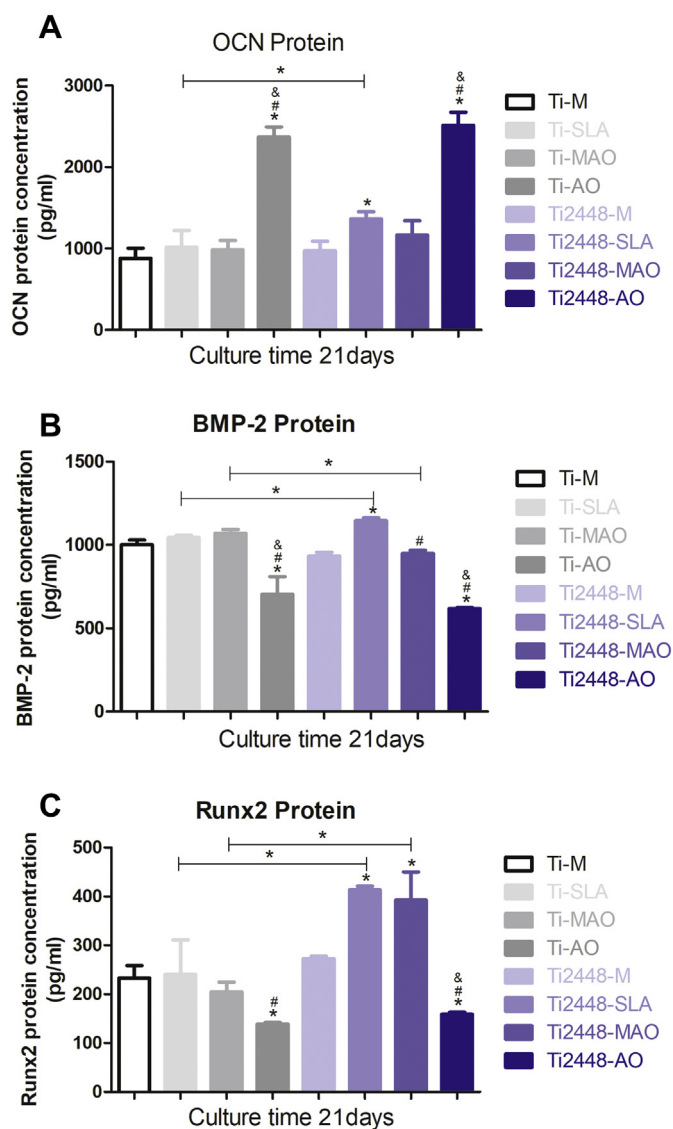


Fig. 10. Relative expression levels of BMP-2, OCN, Runx2 proteins on surfaces modified pure titanium and Ti2448 alloy. Values are presented as mean \pm SD for eight independent cultures. * $p < 0.05$ versus Ti-M and Ti2448-M; # $p < 0.05$ versus Ti-SLA and Ti2448-SLA; & $p < 0.05$ versus Ti-MAO and Ti2448-MAO.

bone tissue and bone bonding on the MAO and AO surfaces *in vivo* are not very clear, which needs to be further studies through *in vivo* experiments, and further efforts need to be made to explore the methods to enhance the bonding strength of the coating and the substrate materials. The effects of elements on bone formation also need to be explored and verified by detailed experiments.

5. Conclusions

After the same surface treatment, the surface morphology of pure titanium and titanium 2448 alloy is obviously different; a micro-structure can be formed by sandblasted, large-grit, acid-etched and micro-arc oxidation, and a nanostructure can be formed by anodic oxidation.

The results for cell proliferation and cell adhesion on the surface of the materials showed the increase of roughness is not conducive to cell growth, but the surface of micro-arc oxidation is opposite.

ALP activity and extracellular matrix mineralization showed that roughness was favorable for cell differentiation, and the surface of

Ti2448 nanostructure with good hydrophilicity was the most favorable for bone formation.

In conclusion, Ti2448 alloy after surface modification has good osteoblast bioactivity, and anodic oxidation is the best method of three surface modifications to further improve bone formation *in vitro*. Ti2448-AO and Ti2448-MAO have potential for clinical application.

Declaration of competing interest

The authors declare that they have no known competing financial interests or personal relationships that could have appeared to influence the work reported in this paper.

Acknowledgements

This work was supported by the National Key Research and Development Program of China (Grant number 2016YFC1102603) and Key Research Program of Frontier Sciences, CAS (Grant number QYZDJ-SSW-JSC031-02).

References

- [1] M. Esposito, J.M. Hirsch, U. Lekholm, P. Thomsen, Biological factors contributing to failures of osseointegrated oral implants. (II). Etiopathogenesis, *Eur. J. Oral Sci.* 106 (1998) 721–764.
- [2] F. De Angelis, P. Papi, F. Mencio, D. Rosella, S. Di Carlo, G. Pompa, Implant survival and success rates in patients with risk factors: results from a long-term retrospective study with a 10 to 18 years follow-up, *Eur. Rev. Med. Pharmacol. Sci.* 21 (2017) 433–437.
- [3] M.S. Tonetti, J. Schmid, Pathogenesis of implant failures, *Periodontology* 2000 4 (1994) 127–138.
- [4] A. Barfeie, J. Wilson, J. Rees, Implant surface characteristics and their effect on osseointegration, *Br. Dent. J.* 218 (2015) E9.
- [5] R.Z. LeGeros, R.G. Craig, Strategies to affect bone remodeling: osteointegration, *J. Bone Miner. Res: The Official Journal of the American Society for Bone and Mineral Research* 8 (Suppl. 2) (1993) S583–S596.
- [6] D.R. Sumner, Long-term implant fixation and stress-shielding in total hip replacement, *J. Biomech.* 48 (2015) 797–800.
- [7] R. Korabi, K. Shemtov-Yona, D. Rittel, On stress/strain shielding and the material stiffness paradigm for dental implants, *Clin. Implant. Dent. Relat. Res.* 19 (2017) 935–943.
- [8] H. Asgharzadeh Shirazi, M.R. Ayatollahi, A. Asnafi, To reduce the maximum stress and the stress shielding effect around a dental implant-bone interface using radial functionally graded biomaterials, *Comput. Methods Biomech. Biomed. Eng* 20 (2017) 750–759.
- [9] M.T. Andani, N. Shayesteh Moghaddam, C. Haberland, D. Dean, M.J. Miller, M. Elahinia, Metals for bone implants. Part 1. Powder metallurgy and implant rendering, *Acta Biomater.* 10 (2014) 4058–4070.
- [10] O.E. Ogle, Implant surface material, design, and osseointegration, *Dental Clin of North America* 59 (2015) 505–520.
- [11] A. Jemat, M.J. Ghazali, M. Razali, Y. Otsuka, Surface modifications and their effects on titanium dental implants, *Biomed. Res. Int.* (2015) 791725.
- [12] M. Xiao, Y.M. Chen, M.N. Biao, X.D. Zhang, B.C. Yang, Bio-functionalization of biomedical metals, *Mater. Sci. Eng. C-Mater. Biol. Appl* 70 (2017) 1057–1070.
- [13] T. Hanawa, Surface treatment and modification of metals to add biofunction, *Dent. Mater. J.* 36 (2017) 533–538.
- [14] N.P. Lang, S. Jepsen, Implant surfaces and design (Working Group 4), *Clin. Oral Implant. Res* 20 (Suppl. 4) (2009) 228–231.
- [15] Krzysztof Rokosz, Tadeusz Hryniewicz, Sofia Gaiaschi, Patrick Chapon, Steinar Raaen, Kornel Pietrzak, Winfried Malorny, João Salvador Fernandes, Characterization of porous phosphate coatings enriched with magnesium or zinc on CP titanium grade 2 under DC plasma electrolytic oxidation, *Metals* 8 (2018) 112.
- [16] T.H. Teh, A. Berkani, S. Mato, P. Skeldon, G.E. Thompson, H. Habazaki, K. Shimizu, Initial stages of plasma electrolytic oxidation of titanium, *Corros. Sci.* 45 (2003) 2757–2768.
- [17] K. Rokosz, T. Hryniewicz, S. Raaen, P. Chapon, Development of copper-enriched porous coatings on ternary Ti-Nb-Zr alloy by Plasma Electrolytic Oxidation, *Int. J. Adv. Manuf. Technol.* 89 (2017) 2953–2965.
- [18] R. Rokicki, T. Hryniewicz, Enhanced oxidation-dissolution theory of electro-polishing, *Trans. Inst. Met. Finish.* 90 (2012) 188–196.
- [19] T. Hryniewicz, R. Rokicki, K. Rokosz, Magneto-electropolishing for metal surface modification, *Trans. Inst. Met. Finish.* 85 (2007) 325–332.
- [20] Tadeusz Hryniewicz, Krzysztof Rokosz, Ryszard Rokicki, Frédéric Prima, Nanoindentation and XPS studies of titanium TNZ alloy after electrochemical polishing in a magnetic field, *Materials* 8 (2015) 205–215.
- [21] R. Rokicki, W. Haider, T. Hryniewicz, Influence of sodium hypochlorite treatment of electropolished and magneto-electropolished nitinol surfaces on adhesion and proliferation of MC3T3 preosteoblast cells, *J. Mater. Sci. Mater. Med.* 23 (2012) 2127–2139.

- [22] R. Junker, A. Dimakis, M. Thoneick, J.A. Jansen, Effects of implant surface coatings and composition on bone integration: a systematic review, *Clin. Oral Implant. Res* 20 (Suppl. 4) (2009) 185–206.
- [23] A. Brizuela, M. Herrero-Climent, E. Rios-Carrasco, J.V. Rios-Santos, R.A. Perez, J.M. Manero, J. Gil Mur, Influence of the elastic modulus on the osseointegration of dental implants, *Materials (Basel, Switzerland)* 12 (2019).
- [24] R. Huiskes, Stress shielding and bone resorption in THA: clinical versus computer-simulation studies, *Acta Orthop. Belg.* 59 (Suppl. 1) (1993) 118–129.
- [25] Y.L. Hao, S.J. Li, S.Y. Sun, C.Y. Zheng, R. Yang, Elastic deformation behaviour of Ti-24Nb-4Zr-7.9Sn for biomedical applications, *Acta Biomater.* 3 (2007) 277–286.
- [26] J. Zhang, S.A.A. Shah, Y. Hao, S. Li, R. Yang, Weak fatigue notch sensitivity in a biomedical titanium alloy exhibiting nonlinear elasticity, *Sci. China-Mater* 61 (2018) 537–544.
- [27] Y. Cheng, J. Hu, C. Zhang, Z. Wang, Y. Hao, B. Gao, Corrosion behavior of novel Ti-24Nb-4Zr-7.9Sn alloy for dental implant applications in vitro, *J. Biomed. Mater. Res. Part B, Applied Biomaterials* 101 (2013) 287–294.
- [28] Y. Bai, Y.L. Hao, S.J. Li, Y.Q. Hao, R. Yang, F. Prima, Corrosion behavior of biomedical Ti-24Nb-4Zr-8Sn alloy in different simulated body solutions, *Mater. Sci. Eng. C-Mater. Biol. Appl* 33 (2013) 2159–2167.
- [29] J. Li, S.J. Li, Y.L. Hao, H.H. Huang, Y. Bai, Y.Q. Hao, Z. Guo, J.Q. Xue, R. Yang, Electrochemical and surface analyses of nanostructured Ti-24Nb-4Zr-8Sn alloys in simulated body solution, *Acta Biomater.* 10 (2014) 2866–2875.
- [30] H. Asgharzadeh Shirazi, M.R. Ayatollahi, A. Asnafi, To reduce the maximum stress and the stress shielding effect around a dental implant-bone interface using radial functionally graded biomaterials, *Comput. Methods Biomech. Biomed. Eng.* 20:7, 750–759.
- [31] E.A. Bonfante, R. Jimbo, L. Witek, N. Tovar, R. Neiva, A. Torroni, P.G. Coelho, Biomaterial and biomechanical considerations to prevent risks in implant therapy, *Periodontology* 2000 81 (2019) 139–151.
- [32] A. Brizuela, M. Herrero-Climent, E. Rios-Carrasco, J.A.-O. Rios-Santos, R.A.-O. Perez, J.M. Manero, J. Gil Mur, Influence of the elastic modulus on the osseointegration of dental implants, *Materials* 12 (2019) 980.
- [33] G. Ryan, D.P. Pandit, A. Fau-Apsatisidis, D.P. Apsatisidis, Fabrication methods of porous metals for use in orthopaedic applications, *Biomaterials* 27 (2006) 2651–2670.
- [34] M. Long, H.J. Rack, Titanium alloys in total joint replacement—a materials science perspective, *Biomaterials* 19 (1998) 1621–1639.
- [35] Z. Guo, J. Fu, Y.Q. Zhang, Y.Y. Hu, Z.G. Wu, L. Shi, M. Sha, S.J. Li, Y.L. Hao, R. Yang, Early effect of Ti-24Nb-4Zr-7.9Sn intramedullary nails on fractured bone, *Mater. Sci. Eng. C*, 29 963–968.
- [36] Y. Qu, S. Zheng, R. Dong, M. Kang, H. Zhou, D. Zhao, J.A.-O. Zhao, Ti-24Nb-4Zr-8Sn alloy pedicle screw improves internal vertebral fixation by reducing stress-shielding effects in a porcine model. *Biomed. Res. Int.* Volume 2018, Article ID 8639648, (13 pages).
- [37] M. Sha, J. Guo Z Fau - Fu, J. Fu J Fau - Li, C.F. Li J Fau - Yuan, L. Yuan Cf Fau - Shi, S.J. Shi L Fau - Li, S.J. Li, The effects of nail rigidity on fracture healing in rats with osteoporosis, *Acta Orthop.* 80 (2009) 135–138.
- [38] Y.J. Park, Y.H. Song, J.H. An, H.J. Song, K.J. Anusavice, Cytocompatibility of pure metals and experimental binary titanium alloys for implant materials, *J. Dent.* 41 (2013) 1251–1258.
- [39] K.C. Nune, R.D. Misra, S.J. Li, Y.L. Hao, R. Yang, Osteoblast cellular activity on low elastic modulus Ti-24Nb-4Zr-8Sn alloy, *Dental Mater: Official Publication of the Academy of Dental Materials* 33 (2017) 152–165.
- [40] K.C. Nune, R.D. Misra, S.J. Li, Y.L. Hao, R. Yang, Cellular response of osteoblasts to low modulus Ti-24Nb-4Zr-8Sn alloy mesh structure, *J. Biomed. Mater. Res. Part A* 105 (2017) 859–870.
- [41] J. Wu, Z.M. Liu, X.H. Zhao, Y. Gao, J. Hu, B. Gao, Improved biological performance of microarc-oxidized low-modulus Ti-24Nb-4Zr-7.9Sn alloy, *J. Biomed. Mater. Res. Part B, Applied biomater* 92 (2010) 298–306.
- [42] Han Xue, Liu Hongchen, Wang Dongsheng, Li Shujun, Y.J. Rui, In vitro biological effects of Ti2448 alloy modified by micro-arc oxidation and alkali heatment, *J.o.M. Science, Technology* 27 (2011) 317–324.
- [43] Y. Hao, S. Li, X. Han, Y. Hao, H. Ai, Effects of the surface characteristics of nanoporous titanium oxide films on Ti-24Nb-4Zr-8Sn alloy on the initial adhesion of osteoblast-like MG-63 cells, *Exp. Ther. Med* 6 (2013) 241–247.
- [44] Y.Q. Hao, S.J. Li, Y.L. Hao, Y.K. Zhao, H.J.J.A.S.S. Ai, Effect of nanotube diameters on bioactivity of a multifunctional titanium alloy, *Appl. Surf. Sci.* 268 (2013) 44–51.
- [45] L. Shi, L. Shi, L. Wang, Y. Duan, W. Lei, Z. Wang, J. Li, X. Fan, X. Li, S. Li, Z. Guo, The improved biological performance of a novel low elastic modulus implant, *PLoS One* 8 (2013) e55015.
- [46] X.H. Liu, L. Wu, H.J. Ai, Y. Han, Y. Hu, Cytocompatibility and early osseointegration of nanoTiO₂-modified Ti-24 Nb-4 Zr-7.9 Sn surfaces, *Mater. Sci. Eng. C-Mater. Biol. Appl* 48 (2015) 256–262.
- [47] X. Li, T. Chen, J. Hu, S. Li, Q. Zou, Y. Li, N. Jiang, H. Li, J. Li, Modified surface morphology of a novel Ti-24Nb-4Zr-7.9Sn titanium alloy via anodic oxidation for enhanced interfacial biocompatibility and osseointegration, *Colloid Surf. B-Biointerfaces* 144 (2016) 265–275.
- [48] C.F. Liu, T.H. Lee, J.F. Liu, W.T. Hou, S.J. Li, Y.L. Hao, H. Pan, H.H. Huang, A unique hybrid-structured surface produced by rapid electrochemical anodization enhances bio-corrosion resistance and bone cell responses of beta-type Ti-24Nb-4Zr-8Sn alloy, *Sci. Rep.* 8 (2018) 6623.
- [49] J.M. Yu, H.-C. Choe, Morphology changes and bone formation on PEO-treated Ti-6Al-4V alloy in electrolyte containing Ca, P, Sr, and Si ions, *Appl. Surf. Sci.* 477 (2010) 121–130.
- [50] F. Rupp, L. Liang, J. Geis-Gerstorfer, L. Scheideler, F. Huttig, Surface characteristics of dental implants: a review, *Dent. Mater.* 34 (2018) 40–57.
- [51] O. Andrukhov, R. Huber, B. Shi, S. Berner, X. Rausch-Fan, A. Moritz, N.D. Spencer, A. Schedle, Proliferation, behavior, and differentiation of osteoblasts on surfaces of different microroughness, *Dent. Mater.* 32 (2016) 1374–1384.
- [52] M.T. Linossier, L.E. Amirova, M. Thomas, M. Normand, M.P. Bareille, G. Gauquelin-Koch, A. Beck, M.C. Costes-Salon, C. Bonneau, C. Gharib, M.A. Custaud, L. Vico, Effects of short-term dry immersion on bone remodeling markers, insulin and adipokines, *PLoS One* 12 (2017) e0182970.
- [53] R.T. Annamalai, P.A. Turner, W.F.t. Carson, B. Levi, S. Kunkel, J.P. Stegemann, Harnessing macrophage-mediated degradation of gelatin microspheres for spatiotemporal control of BMP2 release, *Biomaterials*, 161 (2018), 216–227.
- [54] B.D. Boyan, A. Cheng, R. Olivares-Navarrete, Z. Schwartz, Implant surface design regulates mesenchymal stem cell differentiation and maturation, *Adv. in Dent. Res.* 28 (2016) 10–17.
- [55] R.A. Gittens, L. Scheideler, F. Rupp, S.L. Hyzy, J. Geis-Gerstorfer, Z. Schwartz, B.D. Boyan, A review on the wettability of dental implant surfaces II: biological and clinical aspects, *Acta Biomater.* 10 (2014) 2894–2906.
- [56] E.S. Thian, J. Huang, Z. Ahmad, M.J. Edirisinghe, S.N. Jayasinghe, D.C. Ireland, R.A. Brooks, N. Rushton, S.M. Best, W. Bonfield, Influence of nanohydroxyapatite patterns deposited by electrohydrodynamic spraying on osteoblast response, *J. Biomed. Mater. Res. Part A* 85 (2008) 188–194.
- [57] C. Galli, M. Piemontese, S. Lumetti, F. Ravanetti, G.M. Macaluso, G. Passeri, Actin cytoskeleton controls activation of Wnt/beta-catenin signaling in mesenchymal cells on implant surfaces with different topographies, *Acta Biomater.* 8 (2012) 2963–2968.
- [58] F. Rupp, R.A. Gittens, L. Scheideler, A. Marmur, B.D. Boyan, Z. Schwartz, J. Geis-Gerstorfer, A review on the wettability of dental implant surfaces I: theoretical and experimental aspects, *Acta Biomater.* 10 (2014) 2894–2906.
- [59] A.J.S.M. Marmur, Hydro- hygro- oleo- omni-phobic? Terminology of wettability classification, *Soft Matter* 8 (2012) 6867–6870.
- [60] A. Ghicov, S. Aldabergenova, H. Tsuchiya, P. Schmuki, TiO₂-Nb₂O₅ nanotubes with electrochemically tunable morphologies, *Angewandte Chemie (International ed. in English)* 45 (2006) 6993–6996.
- [61] A.B. Faia-Torres, S. Guimond-Lischer, M. Rottmar, M. Charnley, T. Goren, K. Maniura-Weber, N.D. Spencer, R.L. Reis, M. Textor, N.M. Neves, Differential regulation of osteogenic differentiation of stem cells on surface roughness gradients, *Biomaterials* 35 (2014) 9023–9032.
- [62] Ranj Nadhim Salaie, Alexandros Besinisa, Huirong Led, Christopher Tredwin, Richard D Handy, The biocompatibility of silver and nanohydroxyapatite coatings on titanium dental implants with human primary osteoblast cells, *Mater. Sci. Eng. C-Mater. Biol. Appl* 107 (2020).
- [63] M. Galati, P. Minetola, G. Rizza, Surface Roughness Characterisation and Analysis of the Electron Beam Melting (EBM) Process, *Materials (Basel)* 12 (2019) 2211.
- [64] V. De Bruyn H Fau - Christiaens, R. Christiaens V Fau - Doornewaard, M. Doornewaard R Fau - Jacobsson, J. Jacobsson M Fau - Cosyn, W. Cosyn J Fau - Jacquet, S. Jacquet W Fau - Vervaeke, S. Vervaeke, Implant surface roughness and patient factors on long-term peri-implant bone loss, *Periodontology* 2000 73 (2017) 218–227.
- [65] M. Jacobs R Fau - Quirynen, D. van Steenberghe, R. Naert I Fau - Jacobs, M. Quirynen, Influence of inflammatory reactions vs. occlusal loading on peri-implant marginal bone level, *Adv. Dent. Res.* 13 (1999) 130–135.
- [66] T. Albrektsson, A. Guimond-Lischer, Oral implant surfaces: Part 1—review focusing on topographic and chemical properties of different surfaces and in vivo responses to them, *The Int. J. Prosthodont.* 17 (2004) 536–543.
- [67] V. De Bruyn H Fau - Christiaens, R. Christiaens V Fau - Doornewaard, M. Doornewaard R Fau - Jacobsson, J. Jacobsson M Fau - Cosyn, W. Cosyn J Fau - Jacquet, S. Jacquet W Fau - Vervaeke, S. Vervaeke, Implant surface roughness and patient factors on long-term peri-implant bone loss, *Periodontology* 2000 73 (2017) 218–227.
- [68] M.J. Dalby, N. Gadegaard, R. Tare, A. Andar, M.O. Riehle, P. Herzyk, C.D. Wilkinson, R.O. Oreffo, The control of human mesenchymal cell differentiation using nanoscale symmetry and disorder, *Nature Mater* 6 (2007) 997–1003.